ELSEVIER

Journal of Photochemistry and Photobiology A: Chemistry 110 (1997) 229–234

Journal of PHOTOCHEMISTRY AND PHOTOBIOLOGY A: CHEMISTRY

Detection of benzaldehyde and formaldehyde in the UV photolysis of gas-phase methyl benzoate

Elizabeth Christophy, Kari Myli, Terrance R. Viegut, Jeffrey A. Rzepiela, Jeanne M. Hossenlopp *

Marquette University, Department of Chemistry, P O. Box 1881, Milwaukee, WI 53201-1881, USA

Received 11 September 1996; accepted 25 June 1997

Abstract

The excitation of gas-phase methyl benzoate at 240 nm leads to the observation of phosphorescence. The dispersed phosphorescence spectrum has an assigned origin of 25 270 cm^{-1} and a prominent C=O progression of 1720 cm^{-1}, consistent with literature reports of gas-phase benzaldehyde spectroscopy. Weaker bands, which correspond to formaldehyde ν_{17} and ν_{25}, are also evident. Time-resolved IR diode laser absorption spectroscopy has been used to probe formaldehyde. Excitation of methyl benzoate at 222 nm clearly indicates the generation of formaldehyde as a photoproduct. The temporal profile of the formaldehyde signal is consistent with significant nascent vibrational excitation in this product. The ratio of formaldehyde initially in the ground vibrational state to that in the excited vibrational states is estimated to be 0.6 ± 0.1. The proposed elimination mechanisms are analogous to those postulated for the formation of CO_2 and acetaldehyde from pyruvic acid.

Keywords: Benzaldehyde; Formaldehyde; Methyl benzoate; UV photolysis

1. Introduction

The photochemical reactivity of organic esters is less well understood than that of the corresponding aldehydes and ketones partly due to the shift in the electronic transitions to higher energies. In some cases, the yields of common carbonyl photoinitiated reactions are smaller than those observed for aldehydes and ketones. Norrish type II yields are influenced by the character of the triplet excited state. In general, the $^3(\pi,\pi^*)$ states of aromatic esters [1] are expected [2] to be less reactive with regard to hydrogen abstraction than the $^1(n,\pi^*)$ states. The small quantum yields of the Norrish type II elimination reaction reported [3,4] for the excitation of solution-phase benzoic acid ester derivatives, Ph(CO)OR, may be consistent with this simple picture of triplet state reactivity. Since medium effects are also expected to influence the product yields, studies of gas-phase photochemistry are useful for the determination of the fundamental photochemical reactivity. Important issues in the photochemistry of aromatic esters include the characterization of the low-lying triplet states and the identification of the photoproducts.

There have been a number of spectroscopic studies of alkyl benzoates. Methyl benzoate has been studied in most detail. IR and Raman spectra have been obtained under a variety of experimental conditions [5–7]. Phosphorescence is readily observed in 77 K glasses [8,9], and the lifetimes and vibrational band structure are consistent with the assignment of the emitting state as having $^3(\pi,\pi^*)$ character. Electron spin resonance zero-field splitting parameters also support this assignment [1]. The 0,0 band for the triplet to ground state transition is located at approximately 27 300 cm^{-1} [9]. The origin of the $^1(\pi,\pi^*) \leftarrow S_0$ transition has been determined to be 35 926 cm^{-1} from gas-phase-sensitized phosphorescence excitation [10]. An intense, structureless absorption band at approximately 230 nm has also been identified as being due to a $^1(\pi,\pi^*)$ excited state, although the earliest assignment was an intramolecular charge transfer state [11].

Gas-phase photolysis of methyl benzoate at 266 and 193 nm has been shown to produce the methoxy radical [12]. Previous work in our laboratory has demonstrated that the excitation of gas-phase *n*-alkyl benzoates at 230–245 nm also leads to observable phosphorescence, with emission yields which are strongly dependent on the length of the alkyl chain [13]. The dispersed phosphorescence spectrum observed when methyl benzoate is excited at 245 nm shows a progression in the carbonyl stretching frequency, which is consistent with an emitting state of $^3(n,\pi^*)$ character. The origin is at

* Corresponding author.

1010-6030/97/$17.00
PII S1010-6030(97)00197-4

25 200 cm^{-1}, lower than the $^3(\pi,\pi^*)$ origin observed in methyl benzoate spectra obtained in 77 K glasses [8,9]. The ordering of the undispersed gas-phase phosphorescence yield was observed to be *n*-butyl > methyl > ethyl > *n*-propyl benzoate.

The ordering of the phosphorescence yield as a function of the alkyl chain length suggests that there is at least one competing decay channel. One possibility is Norrish type II elimination. If this elimination channel competes with triplet state emission, the emission yield would be expected to decrease when methyl benzoate is replaced by longer alkyl chain species which can lead to type II products. The trend of decreasing phosphorescence as the alkyl group is changed from methyl to ethyl is consistent with this hypothesis. The rate of initial type II intramolecular hydrogen abstraction [14] increases on going from the abstraction of primary to secondary γ-hydrogen atoms, which is again consistent with the experimental observation of much less phosphorescence originating from *n*-propyl benzoate. Early work on Norrish type II elimination in formate esters [15] follows a trend of type II elimination yields which inversely correlate with the alkyl chain length dependence of the phosphorescence yield. We have recently reported [16] a detailed study of formate ester gas-phase Norrish type II elimination yields. Transient IR absorption spectroscopy was used as an in situ probe of the formic acid produced from a series of six formate esters. Ethyl formate clearly leads to a lower type II elimination yield when compared with *n*-propyl and *n*-butyl formate, however, our results do not support the conclusion that *n*-butyl formate has a lower yield than the ethyl or *n*-propyl case. If benzoates are expected to follow similar trends in type II reactivity, the surprisingly high yield of emission from *n*-butyl benzoate is difficult to reconcile with this simple two-channel picture.

In order to re-examine the effects of molecular structure on *n*-alkyl benzoate ester photophysics and photochemistry, we have initiated a more detailed study of the emission and photoproducts generated from the UV excitation of *n*-alkyl benzoate esters. The focus of this report is the identification of some of the photoproducts obtained from methyl benzoate. Higher resolution phosphorescence measurements demonstrate that the emitting species, in the case of 245 nm excitation of methyl benzoate, is benzaldehyde. The mechanism of benzaldehyde formation is investigated using time-resolved IR diode laser absorption spectroscopy to monitor the production of formaldehyde.

2. Experimental details

The general experimental apparatus used for gas-phase phosphorescence [17] and time-resolved IR diode laser absorption spectroscopy [16] is similar to that described previously. The excitation laser was not focused for any of the studies reported here.

Phosphorescence spectra were obtained using 240 nm excitation. A Questek v-β 2520 excimer laser, operated at 308 nm (XeCl), was used to pump a Lambda Physik FL3002 dye laser at 5 Hz. Coumarin 480 dye was used to obtain 480 nm radiation. The dye laser output was directed through an InRad autotracker which housed a BBO (B-cut) crystal. After separating the fundamental from the second harmonic using a four-prism beam separator, the 240 nm excitation beam was steered through the center of a T-shaped glass sample cell. The UV laser energies used ranged from 0.1 to 1.0 mJ per pulse. The emission was imaged onto the slits of a PTI 1/4 m monochromator using two lenses. Data acquisition was computer controlled as described previously [13,17].

The dependence of the phosphorescence yield on the laser intensity was also explored. The monochromator was set to the peak of the assigned phosphorescence origin, and time-resolved phosphorescence signals were obtained using a LeCroy 9410 digital oscilloscope. Signals were averaged for 100 laser shots and then transferred to a Northgate 386 personal computer for analysis. The laser energy was varied from 0.06 to 0.2 mJ per pulse by attenuation with a series of UV neutral density filters.

For the diode laser experiments, the excimer laser was upgraded to model 2720 in order to permit operation at 222 nm (KrCl). Formaldehyde was probed via the IR transition shown below

$$H_2CO(\nu_2=0, J''_{Ka'',Kc''}=3_{2,1}) + h\nu(1745.9222\ cm^{-1}) \rightarrow H_2CO(\nu_2=1, J'_{Ka',Kc'}=3_{2,1}) \quad (1)$$

The assignment of the formaldehyde probe transition was made using the AFGL HITRAN database [18] to first assign the nearby H_2O transitions. Formaldehyde transitions, such as the probe scheme shown in Eq. (1), were then easily identified using literature assignments [19].

The IR probe and UV excitation laser beams were copropagated through a reaction cell (length, 275 cm) using dichroic mirrors. After passing through the reaction cell, the IR laser was directed through a monochromator and detected using a Judson HgCdTe detector with matched preamplifier. Transient signals were averaged for 1000 UV laser shots using a LeCroy 9410 digital oscilloscope.

Commercial samples of methyl benzoate (Aldrich, 99%) were distilled prior to use. A Hewlett-Packard 5890 gas chromatograph and an HP 5970 mass-selective detector were used for gas chromatography–mass spectrometry (GC–MS) analysis, and proton and ^{13}C nuclear magnetic resonance (NMR) spectra were acquired with a GE GN 300 (300 MHz ^1H, 75 MHz ^{13}C) spectrometer. No trace of contaminants was found in either the GC–MS or NMR analysis of the distilled methyl benzoate sample. After distillation, samples were degassed by multiple freeze–pump–thaw cycles at liquid nitrogen temperature. Neat, flowing ester samples were used for all of the phosphorescence measurements. IR absorption measurements were made with neat samples as well as with flowing mixtures of methyl benzoate and CO_2.

3. Results

The dispersed phosphorescence spectrum obtained from the 240 nm excitation of a 180 mTorr sample of methyl benzoate is shown in Fig. 1. The origin at 25 270 cm^{-1} and the prominent 1720 cm^{-1} progression are unchanged from the results previously [13] reported for 245 nm excitation. Weaker features, not evident in the original lower resolution spectrum, are marked in Fig. 1. One of these features, observed as a shoulder on the low-energy side of each of the main peaks, is shifted by 220 cm^{-1} from the strong progression. The other clear band is located approximately 1190 cm^{-1} from each of the main peaks. No phosphorescence is observed in our apparatus when the excitation wavelength is changed to 222 nm. It should be noted that excitation of ethyl and *n*-propyl benzoate also results in the same origin and prominent progression at 1720 cm^{-1}, although with significantly lower yields and somewhat different relative intensities. Spectral features obtained from the excitation of *n*-butyl benzoate appear to originate from a different electronic state or precursor. Work is in progress to characterize the emission originating from the longer alkyl chain benzoates [21].

Time-resolved IR absorption experiments were performed in order to explore the possibility of H_2CO formation. These experiments were performed at 222 nm, where methyl benzoate absorbs strongly, in order to obtain sufficient photoproduct yield for detection via this technique.

With the diode laser tuned to the peak of the formaldehyde ν_2 $Q(3_{2,1})$ transition, weak transient absorption is observed using methyl benzoate pressures in the 2–8 mTorr range. No change in the transmitted IR intensity under these conditions is observed when the diode laser is tuned away from the formaldehyde probe transition. However, at higher methyl benzoate pressures, the transient signal appears in the "gain" direction rather than absorption. Unlike a true transient gain signal [22], there is also a change in the transmitted IR intensity when the diode laser is tuned away from the formaldehyde probe transition. By subtracting the signal obtained with the diode laser detuned from the probe transition from that obtained with the diode laser tuned to the peak of the transition, a net absorption is observed. These observations are consistent with thermal heating effects due to the strong methyl benzoate absorbance at 222 nm. The addition of a buffer gas causes the off-resonance signal to disappear and transient absorption signals are observed only when tuned to the formaldehyde transition.

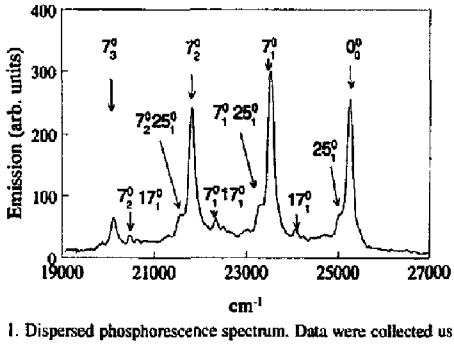

Fig. 1. Dispersed phosphorescence spectrum. Data were collected using a 25 μs gate, delayed 100 μs after the excitation pulse, and 200 laser shots were averaged per wavelength. A flowing 100 mTorr sample of methyl benzoate was used. Benzaldehyde spectral assignments, based on Ref. [20], are labeled.

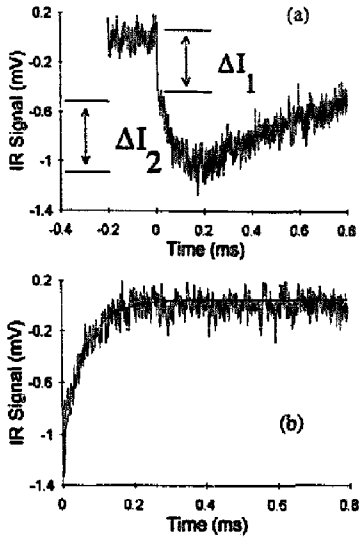

Fig. 2. Transient IR detection of formaldehyde. Data were obtained using a flowing sample of 10 mTorr of methyl benzoate and 800 mTorr of CO_2. The UV laser energy was 2.8 mJ per pulse and the IR I_0 value was 1.7 V. The upper trace shows the raw data. The result after initial long-time exponential curve peeling is shown in the lower panel. The full line through the data in (b) represents the fit to the intermediate time data (see text).

Fig. 2(a) shows a typical transient IR signal obtained using CO_2 as buffer gas. The photolysis laser fires at $t=0$, leading to an immediate absorption of the diode laser probe beam. At times approximately between 10 and 200 μs, there is a continued increase in IR absorption. The IR signal then slowly returns to the pretrigger baseline level.

Data were obtained at different combinations of methyl benzoate and CO_2 pressures in order to characterize the relatively "fast" (ΔI_1) and "intermediate" (ΔI_2) time components of the transient absorption signals identified in Fig. 2(a). In the first step of an exponential curve peeling analysis, the signal was inverted. The return to the baseline for times greater than 0.2 ms was fitted to a single exponential decay. The result of this fit was then subtracted from the entire signal, resulting in plots such as that shown in Fig. 2(b).

The second part of the exponential curve peeling involved fitting the intermediate time data to an exponential rise. Data between 20 and 100 μs were fitted to a single exponential rise with an offset. The dark full line in Fig. 2(b) shows this fit. Extrapolating back to $t=0$ determines the break between the contribution from the initial "fast" increase in absorption and that originating from the slower intermediate time component.

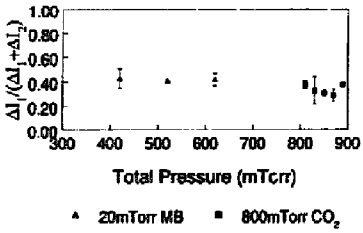

Fig. 3. Initial vs. relaxed IR absorption. The ratio of the initial ground state formaldehyde to the final relaxed population is shown for various methyl benzoate and CO_2 pressures. Signals were not corrected for the upper state transition populations.

Transient IR signals reflect the difference in population between the lower and upper quantum states of the probe transition. The ratio of the initial "fast" absorption to that of the collisionally relaxed population of H_2CO is determined from $\Delta I_1/(\Delta I_1+\Delta I_2)$. This ratio was obtained for 20 mTorr samples of methyl benzoate with 400–600 mTorr of added CO_2. For experiments in which the methyl benzoate sample pressure was varied from 20 to 90 mTorr, the CO_2 pressure was held constant at 800 mTorr, which was necessary to eliminate artifacts from thermal effects at the highest methyl benzoate pressures. Fig. 3 shows the results of these measurements. When the CO_2 pressure is varied, there is negligible variation in the initial to relaxed populations. The average value for these three trials is 0.42 ± 0.05. Greater fluctuation is observed when methyl benzoate pressures are varied, and a slightly lower average, 0.34 ± 0.06, is obtained. These data are not corrected for the upper state population and thus provide a lower bound estimate of 40% vibrational ground state H_2CO initially formed in the reaction.

4. Discussion

The phosphorescence spectrum shown in Fig. 1 correlates well with literature reports [20,23] of the spectrum of gas-phase benzaldehyde. Koyanagi and Goodman [20] reported a value of 25 179.5 cm^{-1} for the origin of the benzaldehyde spectrum and observed a very strong progression at 1728 cm^{-1}, which was assigned to the ν_7 carbonyl stretching mode. The ν_{25} aldehyde in-plane wagging mode at 217 cm^{-1} and the ν_{17} ring mode at 1167 cm^{-1} were observed with moderately strong intensity, consistent with our spectrum. A third moderately strong band, assigned as the 1611 cm^{-1} ν_8 mode, was not evident in our spectrum. The assignment of each of the obvious bands in our spectrum is shown in Fig. 1. The ν_7 intensity profile, uncorrected for instrument response, is also quite similar to the spectrum reported by Hirata and Lim [23], as well as the electron-impact-induced luminescence spectrum of Inoue and Ebara [24].

The original methyl benzoate sample was carefully tested for the presence of benzaldehyde or other impurities, and no trace of any substance other than methyl benzoate was found. Therefore, benzaldehyde is a product which originates from methyl benzoate. There are two possible types of mechanism for benzaldehyde formation. Benzaldehyde could be generated as a secondary product via a bimolecular reaction as shown in Eq. (2a) and Eq. (2b). Formaldehyde could be generated from this scheme via two potential unimolecular decompositions as shown in Eq. (2c) and Eq. (2d). Alternatively, a molecular elimination reaction could lead to the direct production of formaldehyde and either benzaldehyde (Eq. (3)) or the phenyl hydroxycarbene isomer (Eq. (4a)), which might then isomerize to generate benzaldehyde (Eq. (4b)).

$$Ph(CO)OCH_3 + h\nu \rightarrow P\dot{h}CO + OCH_3 \quad (2a)$$

$$P\dot{h}CO + Ph(CO)OCH_3 \rightarrow PhCHO + Ph(CO)O\dot{C}H_2 \quad (2b)$$

$$OCH_3 \rightarrow H + H_2CO \quad (2c)$$

$$Ph(CO)O\dot{C}H_2 \rightarrow P\dot{h}CO + H_2CO \quad (2d)$$

$$Ph(CO)OCH_3 + h\nu \rightarrow PhCHO + H_2CO \quad (3)$$

$$Ph(CO)OCH_3 + h\nu \rightarrow Ph\ddot{C}OH + H_2CO \quad (4a)$$

$$Ph\ddot{C}OH \rightarrow PhCHO \quad (4b)$$

For each of the potential reaction channels, outlined above, it is presumed that benzaldehyde is produced and excited within the 50 ns UV laser pulse. The phosphorescence excitation spectrum reported by Hirata and Lim [23] shows that the excitation of the S_3 state of benzaldehyde at 240 nm leads to strong emission. The excitation spectrum generated from methyl benzoate reported previously [13] is also consistent with the intensity profile of benzaldehyde emission in the 40 000–42 250 cm^{-1} excitation regime. The fact that no emission is observed when 222 nm excitation is used is supported by the very low emission yields in the short-wavelength tail of the S_3 band [23]. These wavelength-dependent trends suggest that benzaldehyde is excited during the laser pulse, rather than directly generated in a triplet state. In addition, the slow (1–5 Hz) UV laser repetition rates and constantly flowing gas mixtures used in our apparatus ensure that the observed emission is generated from species created during the laser pulse, rather than from secondary products which could build up between pulses in a static sample.

The observation of phosphorescence at laser energies lower than 0.1 mJ per pulse with an unfocused laser beam also suggests that methyl benzoate absorbs only one photon. A total of two photons would then be required to generate the observed phosphorescence signals. Laser intensity measurements were performed in order to test this assumption. Time-resolved phosphorescence signals were integrated between 0.045 and 4.0 ms. The formal intensity law [25] derived from the transition rate constant expression for an n-photon process

$$k^{(n)} = \frac{(2\pi)^n \sigma^{(n)} I^n}{(h\omega_r)^n} \quad (5)$$

was used to analyze the experimental data. In Eq. (5), h is Planck's constant, $\sigma^{(n)}$ represents the transition cross-section, I is the laser intensity and ω_L is the laser frequency. An estimate of the number of photons required in a multiphoton process is obtained from a log–log plot of the signal vs. the laser intensity (or energy). Plotting the logarithm of the integrated phosphorescence intensity vs. the logarithm of the laser energy leads to the results shown in Fig. 4. The slope of a least-squares fit to these data is 0.7 ± 0.2, which supports a linear power dependence. This result, although not conclusive, is consistent with the postulated mechanism of the stepwise two-photon process. It is important to note that the formal power law is only strictly valid for non-resonant multiphoton absorption [25]. Molecular dissociation is one of the factors [26] identified as a source of observed power dependences less than the total number of photons required to generate the signal. The analysis of formaldehyde intensity dependences (not shown) is similarly inconclusive.

In the bimolecular reaction mechanism (Eq. (2a) and Eq. (2b)), benzaldehyde is produced from the reaction of a Norrish type I α-cleavage product. The generation of the methoxy radical from methyl benzoate has been demonstrated in this wavelength region [12]. The corresponding second type I product, the PhCO radical, can then abstract a hydrogen atom from methyl benzoate, generating benzaldehyde. For the reaction conditions used here, assuming a collision cross-section of 0.9 nm^2, there is an estimated 5% probability of a collision between a PhCO radical and a methyl benzoate molecule during the 50 ns laser pulse.

The bimolecular channel can be eliminated from further consideration based on energetics. A schematic energy level diagram is shown in Fig. 5. For comparison, a 240 nm photon

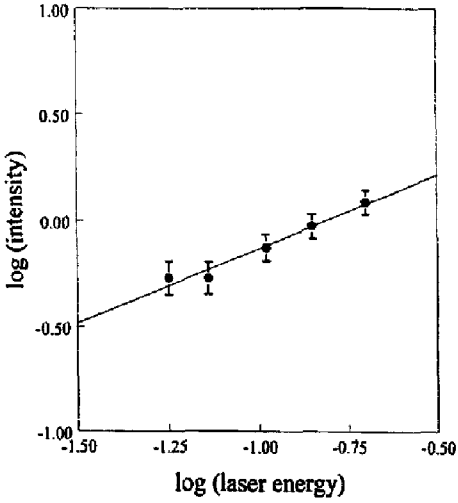

Fig. 4. Laser power dependence of the phosphorescence yields. The logarithm of the integrated phosphorescence intensity vs. the logarithm of the laser energy is shown. Error bars were determined from the uncertainty in fitting the phosphorescence decays using standard propagation of error methods. The result of a least-squares fit to the data ($R^2 = 0.97$) is shown.

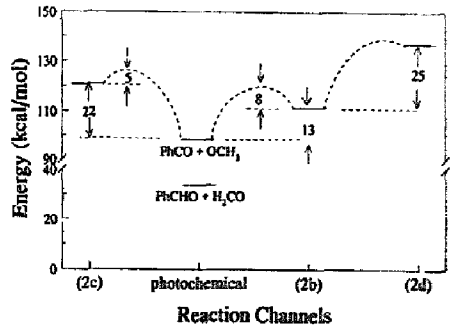

Fig. 5. Energy level diagram. The relative energetics of potential mechanisms for benzaldehyde and formaldehyde formation are shown. Reaction channel labels correspond to the processes defined in the text. The energy levels are determined relative to the ΔH°_f value of the methyl benzoate precursor.

Table 1
Heats of formation

Molecule/radical	ΔH°_f(298 K) (kcal mol^{-1})	Reference
Ph(CO)OCH$_3$	-69 ± 2	[27]
PhCHO	-9 ± 0.5	[27]
H$_2$CO	-26 ± 0.2	[27]
Ph(CO)OCH$_2$	-21 ± 2	[28] [a]
PhCO	30 ± 1	[28] [a]
CH$_3$O	3.7 ± 0.7	[27]

[a] Calculated using tabulated bond energies [28], heats of formation listed above for stable molecules and $\Delta H^\circ_f(H^\cdot) = 52.1$ kcal mol^{-1} [27].

corresponds to 119 kcal mol^{-1}. Table 1 lists the ΔH°_f data [27,28] for the chemical species of interest. The uncertainties in all the energy calculations are determined by the standard propagation of uncertainties reported for the published data. The first step in this mechanism, Norrish type I cleavage (Eq. (2a)), requires 99 ± 2 kcal mol^{-1}, which is feasible at our photolysis wavelengths. Reaction (2b) shown above is endothermic by 13 ± 3 kcal mol^{-1}. Typical activation energies for exothermic hydrogen abstraction reactions involving organic radicals and reactant molecules are of the order of 8 ± 2 kcal mol^{-1} [29]. This allows an estimation of the energetic threshold for the bimolecular reaction channel: approximately 120 ± 6 kcal mol^{-1}. It is unlikely that a process which requires all of the available energy would proceed with sufficient yield to produce the strong phosphorescence signals observed here. Phosphorescence is also observed with good yield using 250 nm (114 kcal mol^{-1}) excitation [13], making it implausible that the bimolecular process is the source of benzaldehyde in these experiments.

The formation of H_2CO from reaction (2d) is also not feasible based on reaction energetics. From the data in Table 1, ΔH°_{rxn} for Eq. (2d) is estimated to be 25 ± 2 kcal mol^{-1}, leading to a minimum energy requirement of 137 kcal mol^{-1}. The value of ΔH°_{rxn} for reaction (2d) is higher than the previously reported value of 17 kcal mol^{-1} [30] due to the use here of more recent ΔH°_f data [27]. The activation energy

for Eq. (2d) has also been estimated to be 26 kcal mol^{-1} [30], which places the threshold for this process at approximately 138 kcal mol^{-1}.

Reaction (2c) is a slightly lower energy pathway for H_2CO production. The barrier for the reverse reaction has been calculated to be 5.6 kcal mol^{-1}, similar to the experimentally determined value of 5.2 kcal mol^{-1} [31]. With a barrier of 5 kcal mol^{-1} for the reverse of reaction (2c), the threshold for H_2CO formation via Eq. (2c) is 126 kcal mol^{-1}. A 222 nm photon corresponds to 129 kcal mol^{-1}. While energetically possible, this channel is inconsistent with the degree of vibrational excitation observed in H_2CO.

Photolysis of OCH_3 must also be considered as a source of H_2CO. The photofragmentation channels of OCH_3 following excitation in the 285–250 nm range have recently been reported [32]. No evidence for $H+H_2CO$ was obtained, although $D+D_2CO$ was observed for the excitation of specific high-energy vibrational transitions. Without experimental data obtained at 222 nm, some secondary photolytic contribution to the H_2CO yield cannot be ruled out.

The best explanation for benzaldehyde and formaldehyde production in these experiments is a molecular elimination mechanism. An analogous reaction is the elimination of CO_2 from pyruvic acid, which has been reported by a number of groups. The formation of a methyl hydroxycarbene intermediate has been suggested as the mechanism for pyruvic acid photodecarboxylation at various wavelengths between 308 and 366 nm [33–35]. The corresponding mechanism has also been proposed for the photolysis of glyoxylic [36] and oxalic [37] acids. The photolysis of pyruvic acid at 193 nm results in substantial vibrational excitation in CO_2 [38–40]. Linear surprisal analysis of the CO_2 vibrational populations supports the direct formation of acetaldehyde at 193 nm [40]. We note that the transient IR profiles of H_2CO obtained here suggest substantial vibrational excitation in this product. However, more information is necessary to identify whether or not the direct elimination channel (Eq. (3)) is the most likely source of benzaldehyde and formaldehyde in this system.

5. Conclusions

Excitation of gas-phase methyl benzoate results in the production of benzaldehyde during the timescale of the laser pulse. Subsequent $S_1 \leftarrow S_0$ excitation of benzaldehyde occurs during the same laser pulse and benzaldehyde emission is observed. The detection of formaldehyde via time-resolved IR absorption spectroscopy supports a molecular elimination mechanism.

Acknowledgements

Support for this work was provided by the National Science Foundation (CHE-9313944).

References

[1] D.R. Arnold, J.R. Bolton, J.A. Pederson, J. Am. Chem. Soc. 94 (1972) 2872.
[2] N.J. Turro, Modern Molecular Photochemistry, Benjamin/Cummings, Menlo Park, CA, 1978, p. 377.
[3] J.A. Barltrop, J.D. Coyle, J. Chem. Soc. B (1971) 251.
[4] M. Day, D.M. Wiles, Can. J. Chem. 49 (1971) 2916.
[5] S. Chattopadhyay, Indian J. Phys. 42 (1968) 335.
[6] D.M. Adams, A. Squire, J. Chem. Soc., Dalton Trans. (1974) 558.
[7] J.H.S. Green, D.J. Harrison, Spectrochim. Acta, Part A 33 (1977) 583.
[8] A.U. Acuna, A. Ceballos, M.J. Molera, J. Chem. Soc., Faraday Trans. 2 72 (1976) 1469.
[9] S.K. Ghoshal, S.K. Sarkar, T.N. Misra, G.S. Kastha, Indian J. Pure Appl. Phys. 17 (1979) 263.
[10] S. Kamei, H. Abe, N. Mikami, M. Ito, J. Phys. Chem. 89 (1985) 3636.
[11] C.J. Seliskar, O.S. Khalil, S.P. McGlynn, in: E.C. Lim (Ed.), Excited States, vol. 1, Academic Press, New York, 1974.
[12] D.E. Powers, J.B. Hopkins, R.E. Smalley, J. Phys. Chem. 85 (1981) 2711.
[13] T.R. Viegut, P.J. Pisano, J.A. Mueller, M.J. Kenney, J.M. Hossenlopp, Chem. Phys. Lett. 195 (1992) 568.
[14] P.J. Wagner, in: P. de Mayo (Ed.), Rearrangements in Ground and Excited States, Academic Press, New York, 1980, pp. 381–444.
[15] P. Ausloos, Can. J. Chem. 36 (1958) 383.
[16] Y. Niu, E. Christophy, P.J. Pisano, Y. Zhang, J.M. Hossenlopp, J. Am. Chem. Soc. 118 (1996) 4181.
[17] V.C. Simianu, H.A. Wilkinson, J.M. Hossenlopp, J. Photochem. Photobiol. A: Chem. 94 (1996) 89.
[18] L.S. Rothman, R.R. Gamache, A. Goldman, L.R. Brown, R.A. Toth, H.M. Pickett, R.L. Poynter, J.-M. Flaud, C. Camy-Peyret, A. Barbe, N. Husson, C.P. Rinsland, M.A.H. Smith, Appl. Opt. 26 (1987) 4058.
[19] D.M. Sweger, R.L. Sams, J. Mol. Spectrosc. 87 (1981) 18.
[20] M. Koyanagi, L. Goodman, Chem. Phys. 39 (1979) 237, and references cited therein.
[21] T.R. Viegut, J.M. Hossenlopp, unpublished results, 1995.
[22] V.C. Simianu, T.R. Viegut, C.M. Lindberg, J.M. Hossenlopp, J. Phys. Chem. 99 (1995) 10 221.
[23] Y. Hirata, E.C. Lim, J. Chem. Phys. 72 (1980) 5505.
[24] A. Inoue, N. Ebara, Chem. Phys. Lett. 109 (1984) 27.
[25] S.H. Lin, Y. Fujimura, H.J. Neusser, E.W. Schlag, Multiphoton Spectroscopy of Molecules, Academic Press, New York, 1984, Chapter 4.
[26] D.H. Parker, in: D.S. Kliger (Ed.), Ultrasensitive Laser Spectroscopy, Academic Press, New York, 1983, Chapter 4.
[27] S.G. Lias, J.E. Bartmess, J.F. Liebman, J.L. Holmes, R.D. Levin, W.G. Mallard, J. Phys. Chem. Ref. Data 17 (Suppl. 1) (1988).
[28] R.C. West (Ed.), CRC Handbook of Chemistry and Physics, 57th ed., CRC Press, Cleveland, OH, 1976–1977, pp. F231–F237.
[29] S. Benson, Thermochemical Kinetics, Wiley, New York, 1968, pp. 100–101.
[30] R.K. Solly, S.W. Benson, Int. J. Chem. Kinet. 3 (1971) 509.
[31] S.P. Walch, J. Chem. Phys. 98 (1993) 3076.
[32] D.L. Osborn, D.J. Leahy, E.M. Ross, D.M. Neumark, Chem. Phys. Lett. 235 (1995) 484.
[33] G.F. Vesley, P.A. Leermakers, J. Phys. Chem. 68 (1964) 2364.
[34] R.N. Rosenfeld, B.R. Weiner, J. Am. Chem. Soc. 105 (1983) 3485.
[35] S. Yamamoto, R.A. Back, Can. J. Chem. 63 (1985) 549.
[36] R.A. Back, S. Yamamoto, Can. J. Chem. 63 (1985) 542.
[37] S. Yamamoto, R.A. Back, J. Phys. Chem. 89 (1985) 622.
[38] C.F. Wood, J.A. O'Neill, G.W. Flynn, Chem. Phys. Lett. 109 (1984) 317.
[39] J.A. O'Neill, T.G. Kreutz, G.W. Flynn, J. Chem. Phys. 87 (1987) 4598.
[40] G.E. Hall, J.T. Muckerman, J.M. Preses, R.E. Weston Jr., G.W. Flynn, Chem. Phys. Lett. 193 (1992) 77.